Wind Rotor Design*

W.A.M. Jansen, P.J. Smulders[†] and E.H. Lysen[†]

Steering Committee, Wind Energy Developing Countries (SWD),
P.O. Box 85, Amersfoort, The Netherlands

ABSTRACT

After a general introduction on wind rotor behaviour and the lift and drag forces on airfoils, a simple method is presented to calculate the blade setting angles and the chords of wind rotors designed for maximum power coefficient.

INTRODUCTION

This article discusses the design of horizontal-axis wind rotors, in which the lift forces on airfoils are the driving forces. Designing a wind rotor basically means choosing a number of parameters, such as the number of blades, the radius of the rotor, the type of airfoil to be used, etc., and to calculate with these parameters the blade setting angle and the chord at each position along the blade.

The choice of the parameters is determined by the type of load that the rotor is expected to drive and by the wind regime at the site where the windmill will be located.

Before going into the details of how to calculate forces on airfoils, a general description of the behaviour of horizontal axis wind rotors will be presented, in which power, torque and speed play a major role.

POWER, TORQUE AND SPEED

A wind rotor can extract power from the wind because it slows down the wind — not too much, not too little. At standstill the rotor obviously produces no power and at very high rotational speeds the air is blocked by the rotor, and again no power is produced. In between these extremes there is an optimal rotational speed where the power extraction is at a maximum. This is illustrated in Fig. 1.

Often one is interested also in the torque-speed curve of a wind rotor, for example when coupling a rotor to a piston pump with a constant torque. The power, P [W], the torque, Q [Nm], and the rotational speed, Ω [rad/s], are related by a simple law:

$$P = Q\Omega \tag{1}$$

With this relation Fig. 2 is found from Fig. 1:

---

* This article is based upon the SWD publication "Rotor Design" by W.A.M. Jansen and P.T. Smulders [1]. The paper has been adapted by E.H. Lysen to form part of a wind energy course given at the Asian Institute of Technology in the summer of 1981.

† Wind Energy Group, Dept. of Physics, Eindhoven University of Technology, the Netherlands.
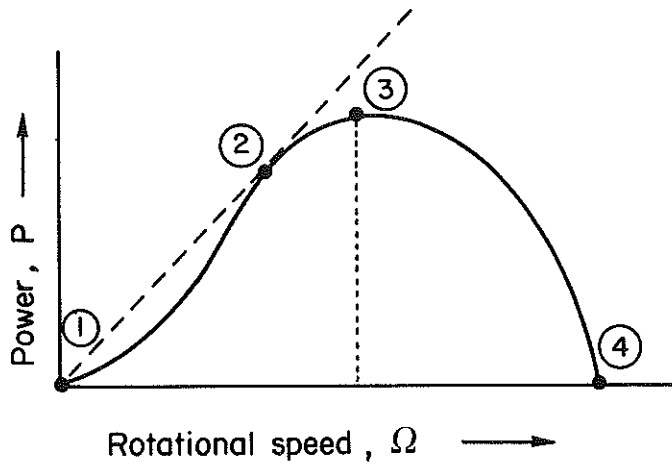
Fig. 1   The power produced by a wind rotor as a function of its rotational speed, at one given wind speed.
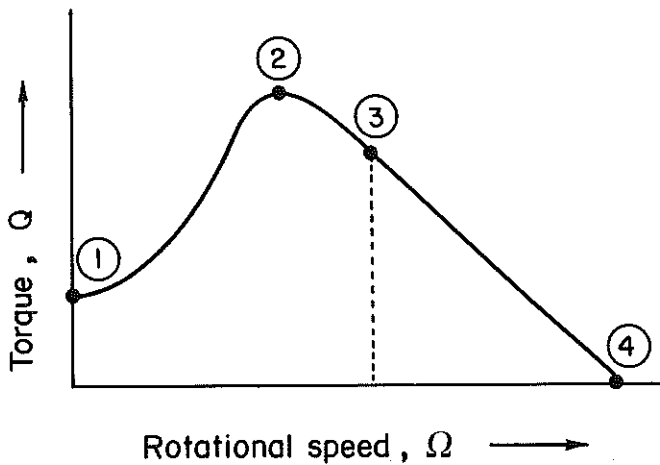

Fig. 2   The torque produced by a wind rotor as a function of its rotational speed at one given wind speed.

One can conclude that because $Q = P/\Omega$, the torque is equal to the tangent of a line through the origin and some point of the P-Ω curve. This is why the maximum of the torque curve is reached at lower speeds than the maximum of the power curve (points 2 and 3 in Figs. 1 and 2).

If the wind speed increases power and torque increase, so for each wind speed a separate curve has to be drawn, both for power and for torque (Fig. 3).

These groups of curves are rather inconvenient to handle as they vary with the wind speed, the diameter of the rotor, and even the density of the air.   Power, torque and speed are made dimensionless with the following expressions:

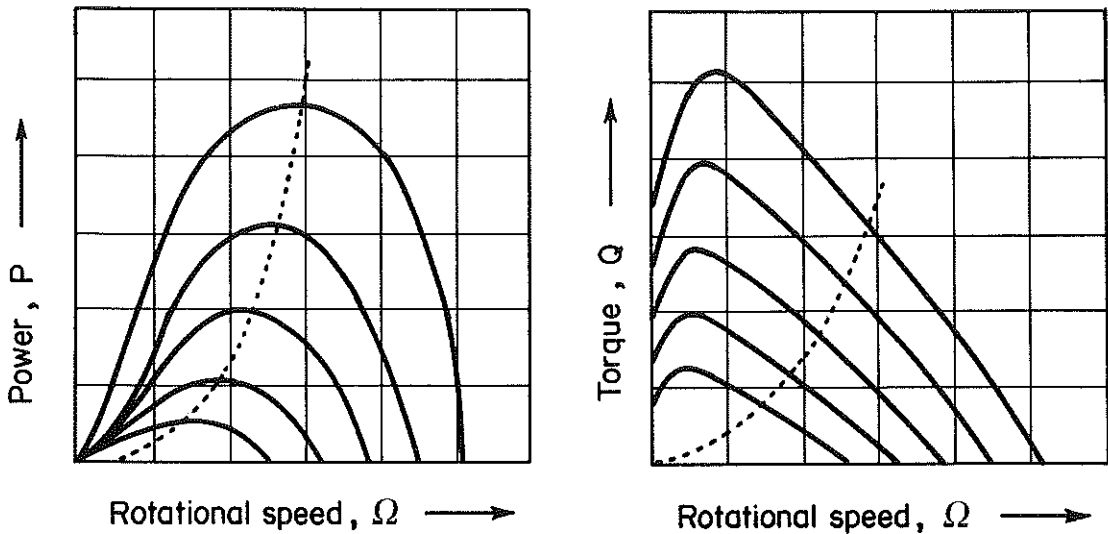$$\text{power coefficient } C_p = P/\tfrac{1}{2}\rho A V^3 \tag{2}$$

Fig. 3   The power and torque of a wind rotor as a function of rotational speed for different wind speeds.

$$\text{torque coefficient } C_Q = Q / \tfrac{1}{2} \rho A V_R^{\,2} \tag{3}$$

$$\text{tip speed ratio } = \Omega R / V \tag{4}$$

where A: swept area of rotor
 R: radius of rotor

Substitution of these expressions in (1) gives:

$$C_p = C_Q \lambda \tag{5}$$

The immediate advantage is that the behaviour of rotors with different dimensions and at different wind speeds can be reduced to two curves: $C_p - \lambda$ and $C_Q - \lambda$

In Fig. 4 the typical $C_p - \lambda$ and $C_Q - \lambda$ curves of a multibladed and a two-bladed wind rotor are shown. One significant difference between these rotors becomes clear: multibladed rotors operate at low tip speed ratios and two- or three-bladed rotors operate at high tip speed ratios. Note that their maximum power coefficient (at the so-called design tip speed ratio $\lambda = \lambda_d$) does not differ all that much, but that there is a considerable difference in torque, both in starting torque (at $\lambda = 0$) and in maximum torque.

An empirical formula to find the starting torque coefficient of a rotor as a function of its optimum tip speed ratio is:

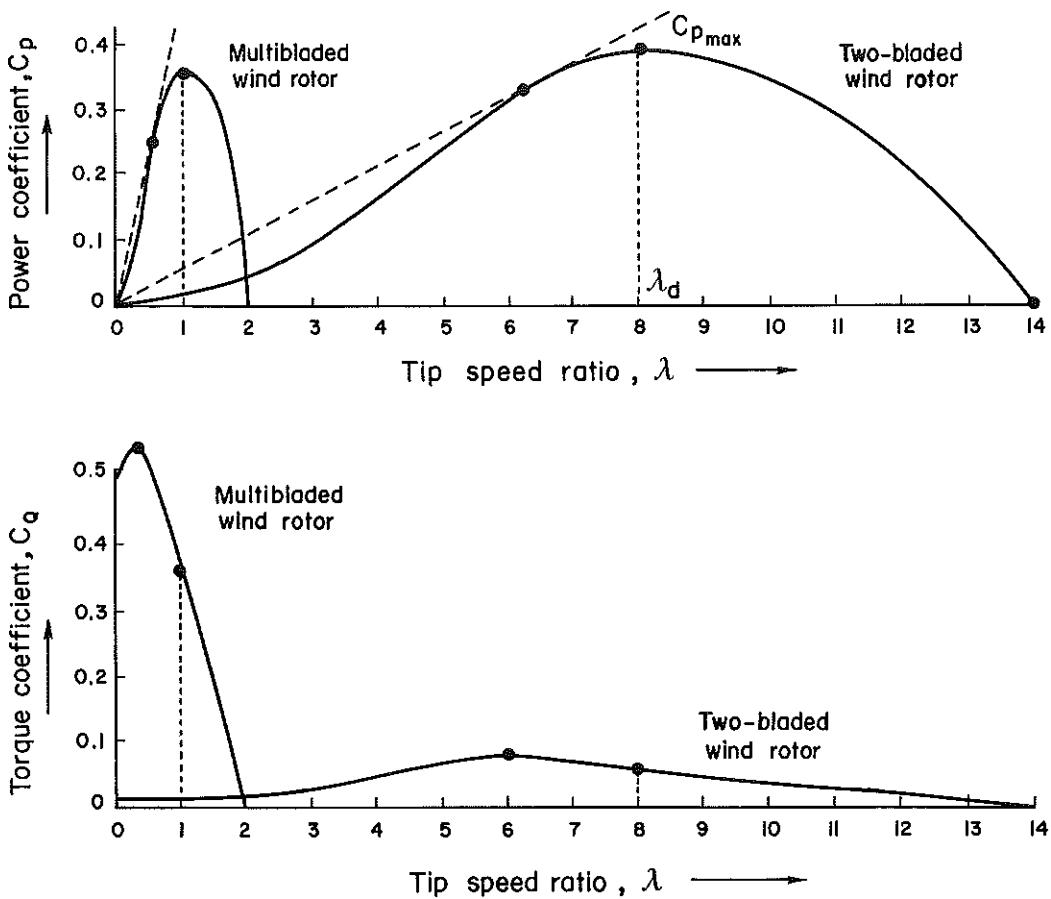$$C_{Q_{start}} = 0.5 / \lambda_d^{\,2} \tag{6}$$

Fig. 4   Dimensionless power and torque curves of two wind rotors as a function of tip speed ratio.

AIR FOILS: LIFT AND DRAG

After having described the rotor as a whole, we turn to the behaviour of the blades in terms of the lift and drag forces on the airfoil-shaped blades.

In fact, not only on airfoils, but on all bodies placed in a uniform flow, a force is exerted, of which the direction is generally not parallel to the direction of the undisturbed flow. The latter point is crucial because it explains why a part of the force, called the *lift*, is perpendicular to the direction of the undisturbed flow. The other part of the force, in the direction of the undisturbed flow, is called the *drag*. For an irregular body and for a smooth airfoil these forces are shown in Fig. 5.

In physical terms the force on a body such as an airfoil is caused by the changes in the flow velocities (and direction) around the airfoil. On the upper side of the airfoil (see Fig. 5) the velocities are higher than on the bottom side. The result is that the pressure on the upper side is *lower* than the pressure on the bottom side, hence the creation of the force, F.
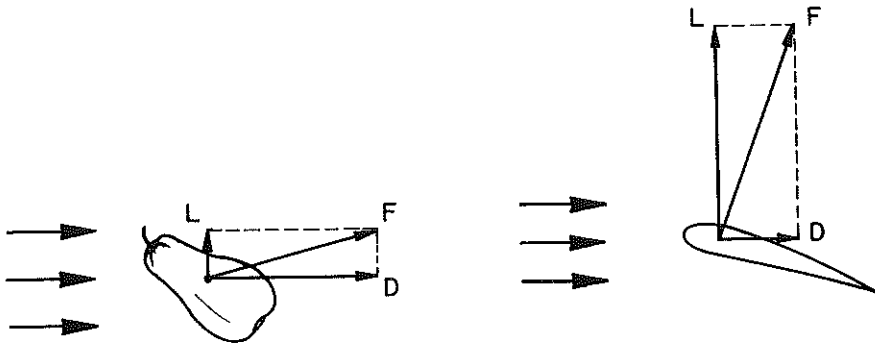
Fig. 5 A body placed in a uniform flow experiences a force, *F*, in a direction that is generally not parallel to the undisturbed flow. The actual direction of *F*, and therefore the sizes of its two components, lift and drag, strongly depends on the shape of the body.

What is the role of the lift and drag forces in the behaviour of the blade of a horizontal-axis wind rotor? To answer that question, we can draw a cross section of the blade, looking from the tip to the root of the blade (Fig. 6).
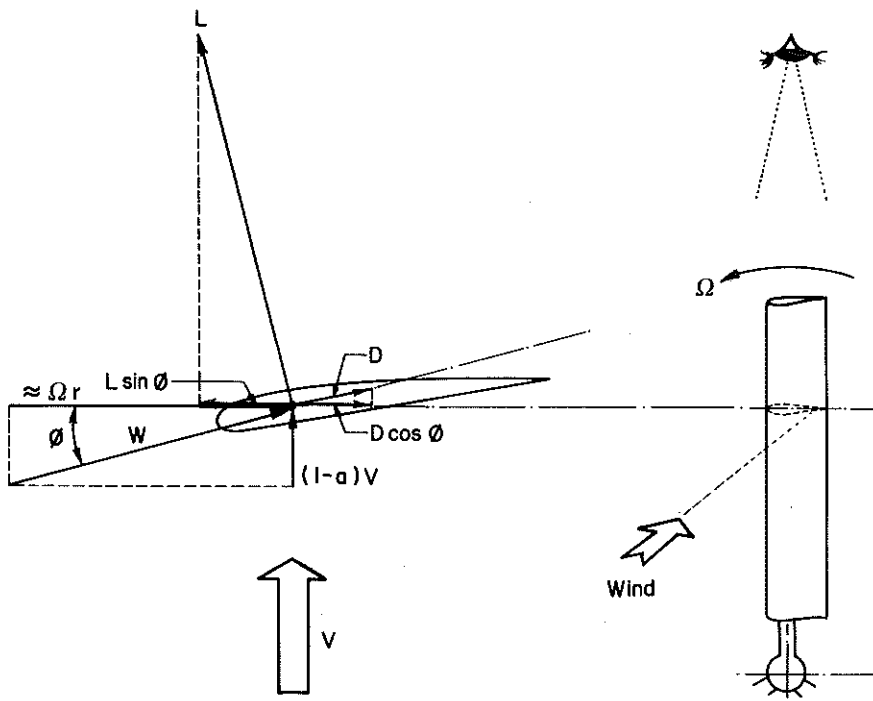

Fig. 6 The driving force to a horizontal axis wind rotor is the forward component, $L \sin \phi$ of the lift, reduced by the backward component, $D \cos \phi$ of the drag.

We see that the relative wind speed, W, which is "felt" by the blade, is composed of two parts: 1. the original wind speed, V, but slowed down to a value $(1- a) V$ as a result of the power extraction, and 2. the wind speed, Ωr, due to the rotational speed, Ωr, of the blade itself, in a direction opposite to the direction of movement.* The angle between the relative wind speed, W, and a reference line of the airfoil is called the *angle of attack*, α. The reference line of the airfoil can be defined as the line touching the outermost point of the airfoil, or as the line connecting the tailing edge (at the back) with the center of the smallest radius of curvature at the leading edge, or the "nose" of the airfoil (see Fig. 10).

The lift force, L, is by definition perpendicular to W, and D is parallel to W. The actual driving force is the component $L \sin\phi$ of the drag. One immediately sees the importance of utilising airfoils with a high lift and a low drag.

When comparing the lift and drag properties of airfoils, one usually refers to the dimensionless lift and drag coefficients, which are defined as follows:

$$\text{lift coefficient } C_L = L / \tfrac{1}{2} \rho V^2 A \qquad (7)$$

$$\text{drag coefficient } C_D = D / \tfrac{1}{2} \rho V^2 A \qquad (8)$$

where ρ : density of air [kg/m^3]
V : undisturbed wind speed [m/s]
A : projected blade area (i.e. chord x length) [m^2]

The values of C_L and C_D vary with the Reynolds number, but we will neglect this influence here and assume that we possess the curves of C_L and C_D as a function of α for the proper Reynolds number. An example of a $C_L - \alpha$ curve and also of a $C_L - C_D$ curve with α as the parameter is shown in Fig. 7.
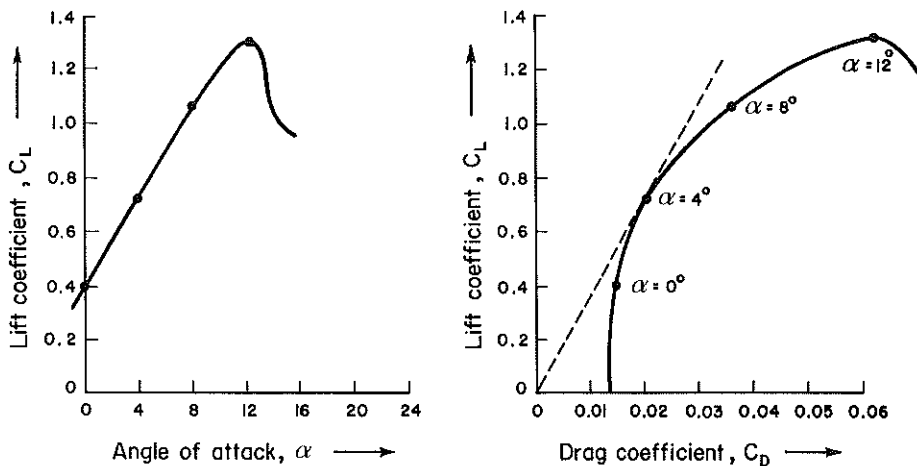

Fig. 7 The lift and drag coefficient of a given airfoil.

---

* In reality, the windspeed, Ωr, is increased with a small component, $\tfrac{1}{2} \omega r$, due to the rotation of the wake with a rotational speed, ω.

The tangent to the $C_L - C_D$ curve drawn from the origin indicates the angle of attack with the maximum C_D/C_L ratio. This ratio strongly determines the maximum power coefficients that can be reached, particularly at high tip speed ratios, as explained in the next paragraph.

The values of α and C_L at minimum C_D/C_L ratio are important parameters in the design process. The values for some airfoils are given below:

Table 1

Typical values of the drag-lift ratio C_D/C_L and of α and C_L for a number of airfoils. The curvature of the curved plate profile is defined as the ratio of its projected thickness and its chord.

		C_D/C_L	α	C_L
Flat plate	—	0.1	5°	0.8
Curved plate (10 % curvature)		0.02	3°	1.25
Curved plate with tube on concave side		0.03	4°	1.1
Curved plate with tube on convex side		0.2	14°	1.25
Airfoil NACA 4411		0.01	4°	0.8

THE MAXIMUM POWER COEFFICIENT

It has been shown by Betz (1920), with a simple axial momentum analysis, that the maximum power coefficient for a horizontal axis type wind rotor is equal to 16/27 or 59.3%. This, however, is the power coefficient of an ideal wind rotor with an infinite number of (zero-drag) blades. In practice there are three effects which cause a further reduction in the maximum attainable power coefficient, namely:

1. the rotation of the wake behind the rotor;
2. a finite number of blades; and,
3. a C_D/C_L ratio larger than zero.

The creation of a rotating wake behind the rotor can be understood by imagining oneself as moving with the wind towards a multibladed wind rotor at standstill (Fig. 8). The passage of the air between the rotor blades causes the blades to start moving to the left (for example), but the air flow itself is deflected to the right (in fact this deflection *causes* the lift). The result is a rotation of the wake, implying extra kinetic energy losses and a lower power coefficient.

For wind rotors with higher tip speed ratios, i.e. with smaller blades and a smaller angle of attack (as we will see later), the effect of wake rotation is much smaller. For infinite tip speed
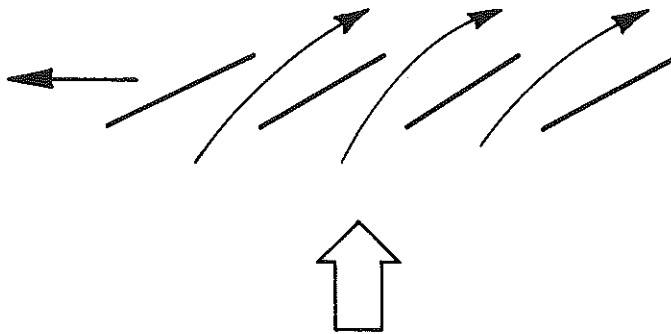
Fig. 8   The creation of a rotating wake behind a wind rotor.

ratios the Betz coefficient could be reached, were it not for the other two effects which come into play.

A finite number of blades, instead of the ideal infinite blade number, causes an extra reduction in power, particularly at low tip speed ratios. This is caused by the pressure leakage around the tip of the blade: the higher pressure at the lower side of the airfoil and the lower pressure at the upper side are "short circuited" at the tip of the blade, causing a crossflow around the tip, hence a decrease in pressure difference over the airfoil, and a lift force approaching zero at the tip itself. The length-width ratio of the whole blade determines the influence of this tip loss, which is why an infinitely small blade has no tip losses. To design a rotor with a given tip speed ratio, one can choose between many blades with a small chord width or less blades with a larger chord.
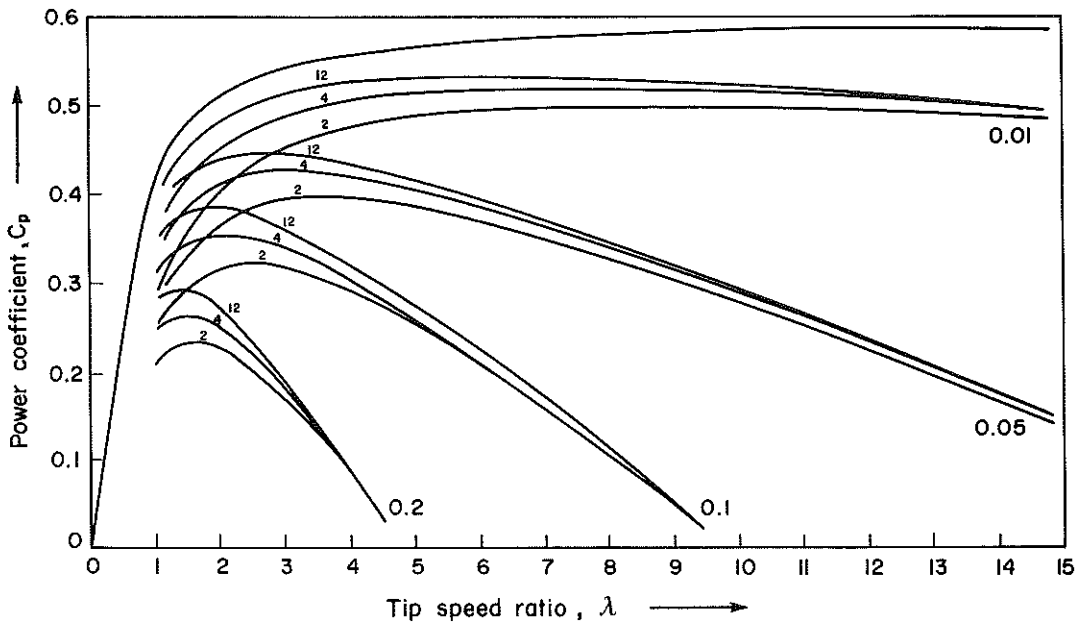

Fig. 9. The influence of blade number and lift/drag ratio on the maximum attainable power coefficient for each tip speed ratio.

With this in mind, it will be clear that for a given tip speed ratio, a rotor with less blades will have larger tip losses. Since the chords become smaller for high tip speed ratios, this effect is smaller for higher tip speed ratios (Fig. 9).

The last effect is the drag of the profile, characterized by the C_D/C_L ratio of the airfoil. This causes a reduction of the maximum power coefficient that is proportional to the tip speed ratio and to the C_D/C_L ratio. The result is shown in Fig. 9. It must be stressed that these curves are *not* $C_p - \lambda$ curves, but $C_{p(max)} - \lambda$ curves. They show for each λ the maximum attainable power coefficient, with the blade number and the C_D/C_L ratio as a parameter.

DESIGN OF THE ROTOR

The design of the rotor consists in finding values of the chord, c, and the setting angle, β, (Fig. 10) of the blades, both at a number of positions along the blade. The calculations that follow are valid for a rotor operating at its maximum power coefficient, also called the "design" situation of the rotor. The values of λ, C_L and α in this situation are referred to as λ_d, C_{L_d} and α_d.
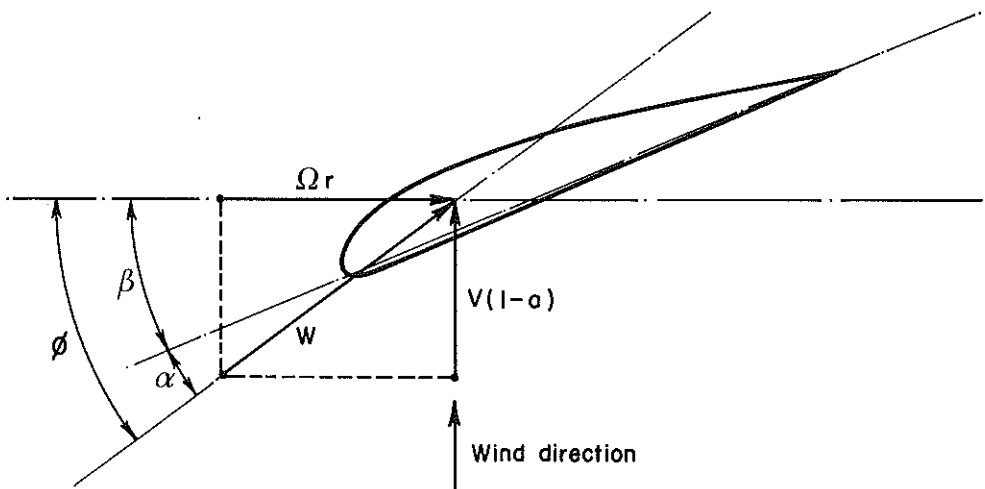

Fig. 10. The angle of attack, α, and the setting angle, β, of the blade of a wind rotor.

One must choose values for the following parameters beforehand:

$$\text{Rotor} \begin{cases} R & : \quad \text{the radius} \\ \lambda_d & : \quad \text{the design tip speed ratio} \\ B & : \quad \text{number of blades} \end{cases}$$

$$\text{Airfoil} \begin{cases} C_{L_d} & : \quad \text{design lift coefficient} \\ \alpha_d & : \quad \text{corresponding angle of attack} \end{cases}$$

The radius of the rotor must be calculated with the required energy output in a year (or in

a critical month), given the average local wind speed, V, and its distribution. A simple approximation for water pumping windmills is given by:

$$E = 0.1\,\pi R^2 V^3 T \qquad [\text{Wh}] \qquad (9)$$

with T : period length in hours

This approximation is reasonable in situations where one has chosen a design wind speed equal to the average wind speed: $V_d = V$. For electricity generating wind turbines the factor 0.1 can be increased to 0.15, or sometimes to 0.2 for very efficient machines.

The choices of λ_d and B (number of blades) are more or less related, as the following guidelines suggest:

Table 2
Guidelines for the choice of the design tip speed and the number of blades.

λ_d	B
1	6 – 20
2	4 – 12
3	3 – 6
4	2 – 4
5 – 8	2 – 3
8 – 15	1 – 2

The type of load will determine λ_d: water pumping windmills have $1 < \lambda_d < 2$, and electricity generating wind turbines usually have $4 < \lambda_d < 10$.

The airfoil data are selected from Table 1.

Four formulas now describe the required information about β and c:

$$c = \frac{8\pi r}{BC_{L_d}}\,(1\text{-}\cos\phi) \qquad (10)$$

$$\beta = \phi - \alpha \qquad (11)$$

$$\phi = \frac{2}{3}\arctan\frac{1}{\lambda_r} \qquad (12)$$

$$\lambda_r = \lambda_d - \frac{r}{R} \qquad (13)$$

The design procedure will be described with the help of an example, in this case of a rotor designed by A. Kragten of the Eindhoven University of Technology, in the programme for the Steering Committee Wind Energy Developing Countries, the Netherlands. The rotor is designed to drive a reciprocating piston pump.

$$R = 1.37$$
$$B = 6$$
$$\lambda_d = 2$$
$$C_{L_d} = 1.1 \quad \left.\begin{array}{l}\end{array}\right\} \text{ Curved plate profile (10\% curvature)}$$
$$\alpha_d = 4° \quad \text{with tube in concave side (see Table 1)}$$

The procedure is straightforward if one decides to keep the lift coefficient at a constant value of C_{L_d}. In that case, a varying chord and varying setting angle, β, will result. If one wishes to design a blade with a constant chord (for ease of production for example) then the lift coeffi- ceint will vary along the blade. We will discuss these two possibilities, keeping in mind that many other alternatives exist.

Constant lift coefficient

The procedure consists of calculating the chord, c, and setting angle, β, at a number of posi- tions along the blade, each with a distance, r, to the rotor axis and a local tip speed ratio, λ_r. In our case, four positions are chosen and for each position the relevant parameters are calculated with the formulas (10) to (13) and presented in Table 3 and Fig. 11.

Table 3
Calculation of chord and setting angle for a six-bladed rotor, ϕ 2.74 m, with a constant lift coefficient

Position	r (m)	λ_r	ϕ	α_d	β	c (m)
1	0.34	0.5	42.3°	4°	38.3	0.337
2	0.68	1.0	30.0°	4°	26.0	0.347
3	1.03	1.5	22.5°	4°	18.5	0.298
4	1.37	2	17.7°	4°	13.7	0.247

One can see in Fig. 11 that the chord of the blade is continuously varying along the blade. Also the setting angle varies, and this "twist" does not vary linearly along the blade. Both factors prevent an easy manufacture of this blade, and it is natural to look at ways to deviate from this shape without sacrificing too much of its performance. One approach is the constant chord blade.

Constant chord

Looking at formula (10) one sees that now the lift coefficient at the different positions along the blade will vary.
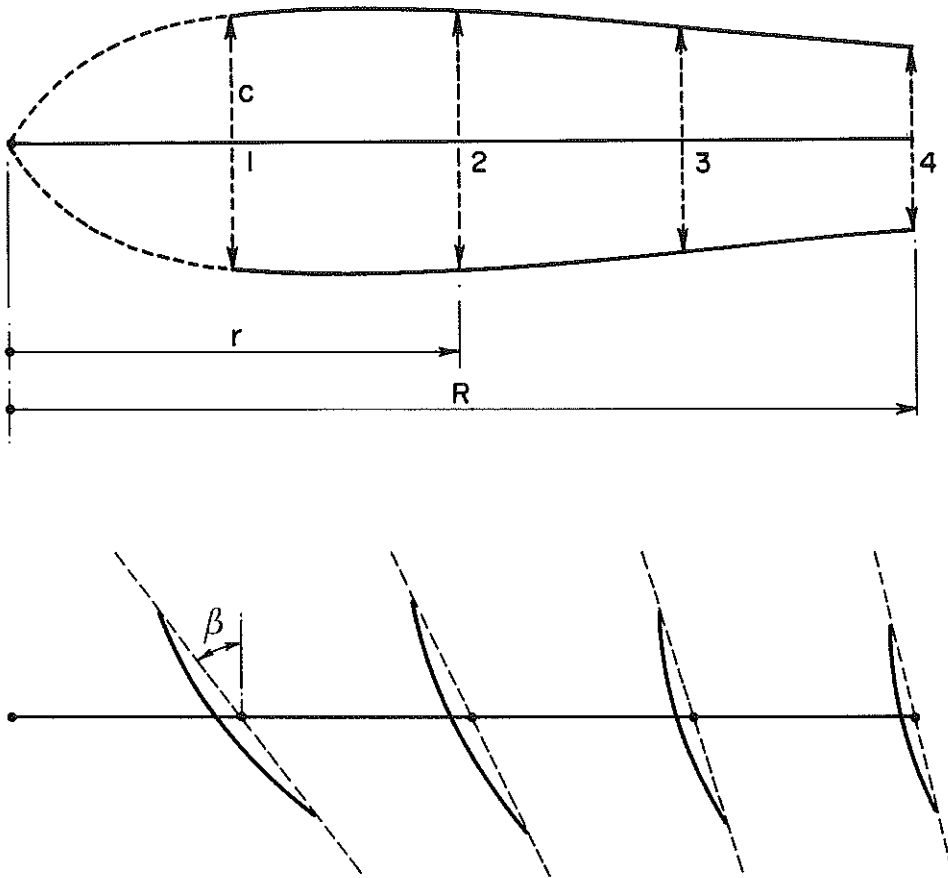
Fig. 11 Blade shape and setting angles at four positions along the blade.

$$C_L = \frac{8\pi r}{Bc}(1 - \cos\phi) \tag{14}$$

Because variations in lift coefficient can only be accomplished via variations in the angle of attack, a fifth relation is needed in addition to our set of four equations, (10) to (13). The relation is:

$$C_L = C_L(\alpha) \tag{15}$$

The $C_L(\alpha)$ graph for the profile in our example is given in Fig. 12.

In the case of the rotor in our example, the dimensions of the blade were dictated by the standard sheet sizes: six blades had to be cut from a sheet of 1 x 2 m with a minimum loss. As a result, our uncurved blade measures 0.333 x 1 m, and the curved blade (10% curvature) has a chord of 0.324 m.
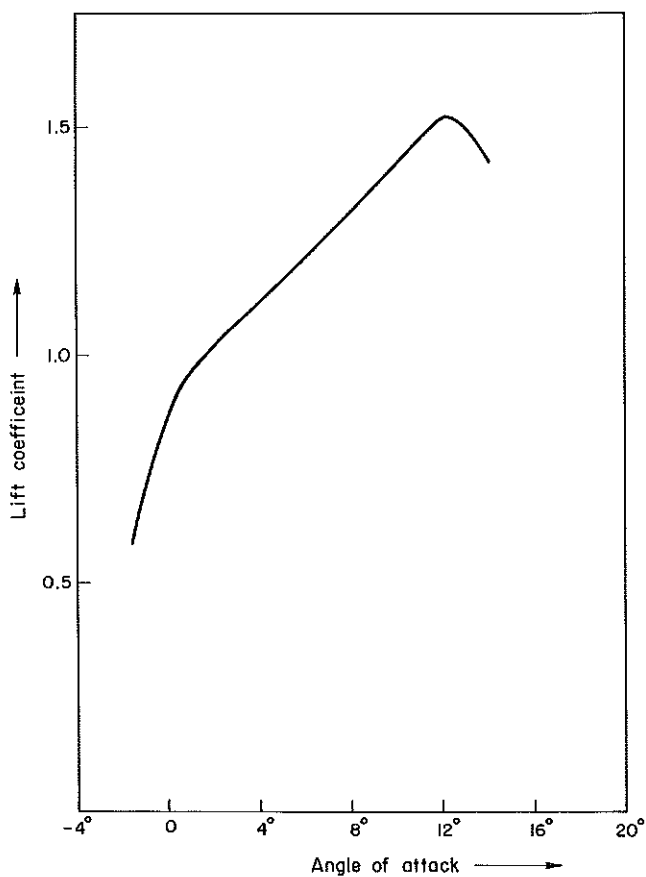
Fig. 12 The lift coefficient of a curved plate (10% curvature) with a tube in the middle of the concave side, at
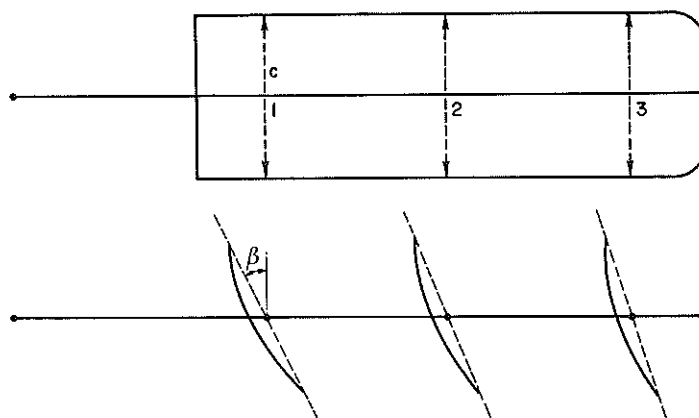Re = 2 x 10^5 (Schumack, 1979).

Fig. 13 Blade shape and setting angles of a blade of the six-bladed wind rotor.

The positions chosen for the calculation were the positions of the 3 struts to fix the blade to the tube, and are presented in Table 4 below. The final shape of the blade is given in Fig. 13.

Table 4

Calculation of lift coefficient, angle of attack, and setting angle for the constant chord blade of a six-bladed rotor, ϕ 2.74 m

Position	r (m)	λ_r	ϕ	c (m)	C_L	α	β	Chosen β
1	0.50	0.73	35.9°	0.324	1.23	6.4°	29.5°	27°
2	0.86	1.26	25.7°	0.324	1.10	3.6°	22.1°	23°
3.	1.22	1.78	19.6°	0.324	0.91	0.2°	19.3°	19°

One notes in Table 4 that the setting angle finally chosen differs from the theoretical angle. This is because it is very difficult to manufacture a curved plate blade with a non-linear twist.

So starting from the correct angle nearby the tip, a good compromise is sought so as to keep the same change in angle between positions 1 and 2 and between positions 2 and 3. Also integer values for the angles are chosen.

The performance of the constant chord rotor has been measured with a rotor model, scaled down to ϕ 1.5 m, and tested in the outlet of an open wind tunnel, ϕ 2.2 m. The resulting $C_p - \lambda$ curve is shown in Fig. 14.
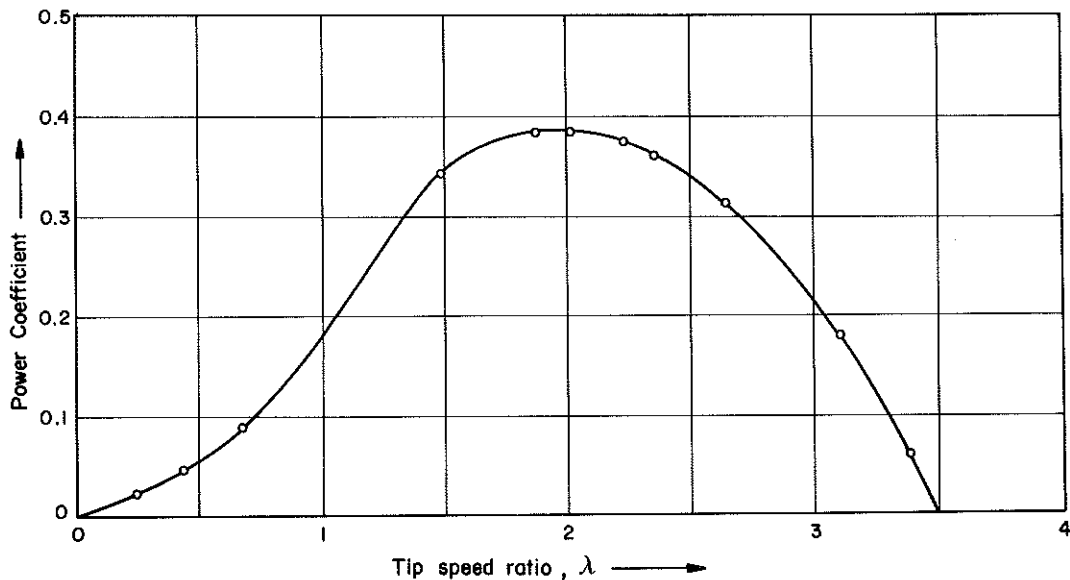

Fig. 14 Performance of the constant chord rotor in the wind tunnel.

REFERENCES

1.   JANSEN, W.A.M. and P.T. SMULDERS (1977), *Rotor Design for Horizontal Axis Wind-mills,* Steering Committee Wind Energy Developing Countries, SWD 77-1, May 1977.

2.   SCHUMACK, M. (1979), *Results of Wind Tunnel Tests on the Scale Model of THE 1/2 Rotor,* Internal report (R 408 S), Wind Energy Group, Department of Physics, Eindhoven University of Technology, December 1979.